

Photo Degradation of Congo Red Dye by Using New Nanocomposite

Entisar E. Al-Abodi^{1a}, Afrah Hashim¹

¹College of Education Ibn Al-Haitham, Chemistry Department, University of Baghdad, Baghdad, Iraq

^aentisaree2020@gmail.com

Abstract: This studied is directed to water treatment by using developed self-assembly method by prepared a TFGO nanocomposite from limited amounts of Titanium dioxide nanoparticles, Iron oxide nanoparticles & Graphene oxide nanosheets. The producing material used as catalyst by applying it in advanced oxidation processes (AOP) to degradation of Congo Red (CR) dye under solar light and that showed excellent synergy between photocatalysis and Fenton-like reactions. The prepared catalyst is stable over a wide range of temperatures, and can be easily extracted from solution and repeatedly used with little loss of catalytic activity. The photodegradation activity could be gained 93% at existence of TFGO nanocomposite as photocatalyst within 600 min.

Keywords: photocatalysts, AOP, TFGO nanocomposite, Congo Red (CR) dye

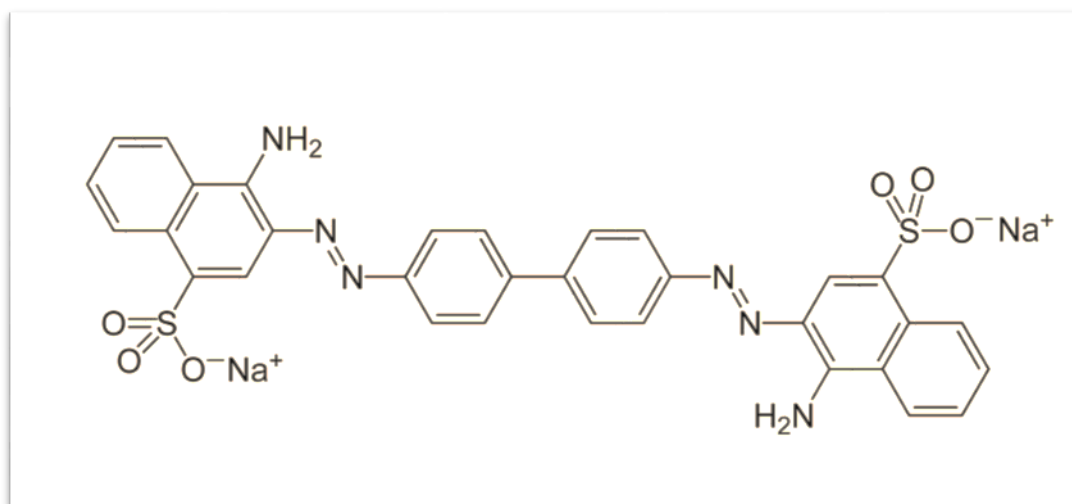
1.Introduction

Methods such as adsorption and flocculation have been used to remove dye pollutants from wastewater (1,2) although many such treatment methods do not clean the pollutants totally and can produce secondary waste products which require further processing (3). Of note though is that chemical oxidation, or the conventional Fenton process, is one of the most efficient, low cost and convenient advanced oxidation processes for water treatment (4,5), Photocatalysis is an advanced oxidation (AOP) process which is applied for degradation of diverse pollutant under solar light. So, it is more desired to prepare photocatalysts that can worked efficiency under natural light.

Among several photocatalysts, titanium dioxide (TiO₂) is a semiconductor, and it is the particularly suitable material for common applications such as energy storage, photocatalysis and wide range of environmental applications[6]. TiO₂ is an environmental-friendly material, non-toxic, stable in aqueous solutions, relatively inexpensive, strong oxidizing power, having high chemical inertness, high thermal stability and photostability [7,8].

In this research, (TFGO) nanocomposite (consist of different amounts of GO nanosheets, F₃O₄, and TiO₂ nanoparticles) was prepared by using a self-assembly way at normal conditions. The efficiency of the TFGO

composite for the Congo Red (CR) dye degradation is studied and the related photo-Fenton degradation and mineralization mechanisms are discussed. Having removed the dye, (TFGO) nanocomposite was removed by the magnetic separation. Congo Red [9], IUPAC name is sodium salt of 3,3'-([1,1'-biphenyl]-4,4'-diyl)bis(4-aminonaphthalene-1-sulfonic acid). (A molecular formula $C_{32}H_{22}N_6Na_2O_6S_2$, molecular structure as in figure 1, and the molar mass is 696.66 g/mol $\text{g}\cdot\text{mol}^{-1}$), which used in our research were obtained from BHD.



Figure(1): The molecular structure of Congo red dye

2. Experimental

2.1 TFGO nanocomposite Preparation

A- The Chemical: iron(II) sulphate heptahydrate ($\text{FeSO}_4 \cdot 7\text{H}_2\text{O}$, 98%), Iron(III) chloride anhydrous (FeCl_3 , $\geq 97\%$, Sinopharm Chemical), Sodium hydroxide (NaOH , 99%, Applichem GmbH, Germany), Hydrochloric acid (HCl , 37%, ROMIL-SA), concentrated Sulphoric acid (H_2SO_4 Sigma Aldrich), graphite, NaNO_3 (Sigma Aldrich), KMnO_4 (Sigma Aldrich). The anatase TiO_2 nanoparticles were purchased from Hongwu International Group Ltd- China, and their size is about 30nm-50nm. The materials used here without any purification.

B- (TFGO) Nanocomposite Fabrication

The graphene oxide (GO) nanosheets were prepared by using a modified Hummers way [10]. FGO and TFGO nanocomposites were obtained by

self-assembly method according to the a literature[4], and we used TiO₂ nanoparticles instead of ZnO nanoparticles .

2.2. The Photocatalysis Activity

The photocatalytic activity of the prepared catalyst (TFGO nanocomposite) were evaluated with sun light as UV irradiation source by photocatalytic degradation in CR aqueous solution. During all experiments of CR dye degradation, the temperature was (35C). eight samples contain (0.05g) of catalysts (TFGO nanocomposite) was added to the 50 ml of (10 ppm) CR solution, and they shaking at 100 cycle min⁻¹ in the dark for 70 min to reach the adsorption-desorption equilibrium (shown in Fig. S2) before the catalytic activity test. Subsequently, the heterogeneous Photocatalytic process was started when the samples was putted under sun radiation and of catalysts (TFGO nanocomposite) was added. Then , the samples were withdrawn at limited time intervals and the Photocatalysis were removed by the magnetic separation, and the residual CR dye concentration was determined by using Visible spectroscopy at 497 nm[4].

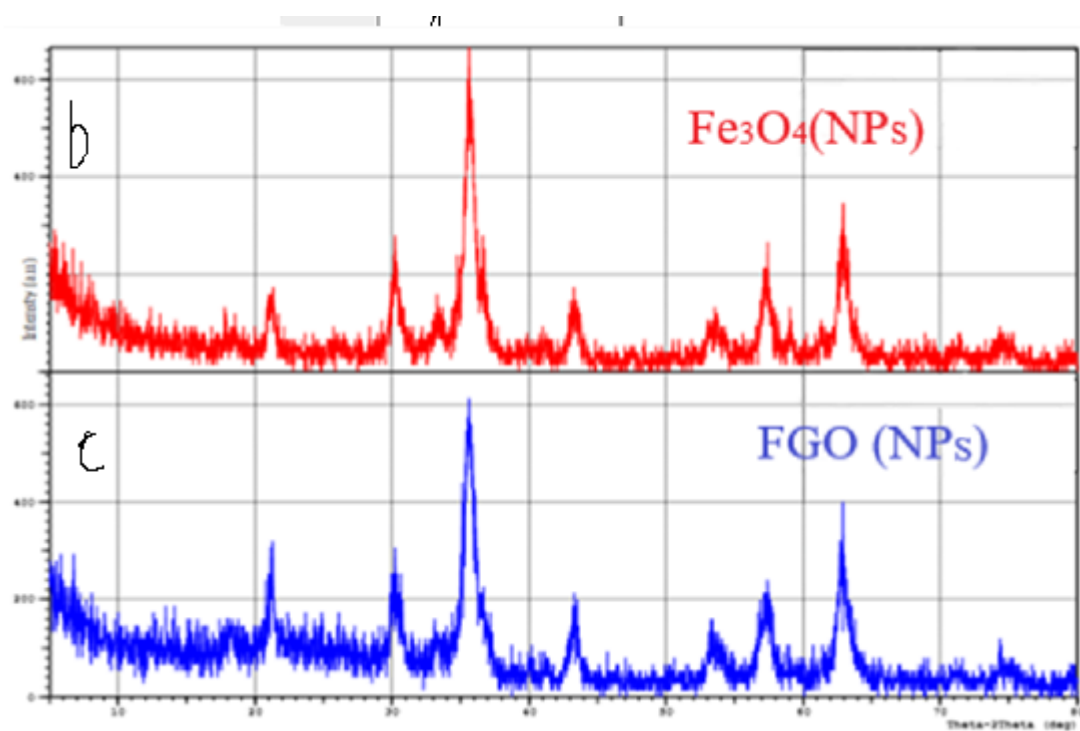
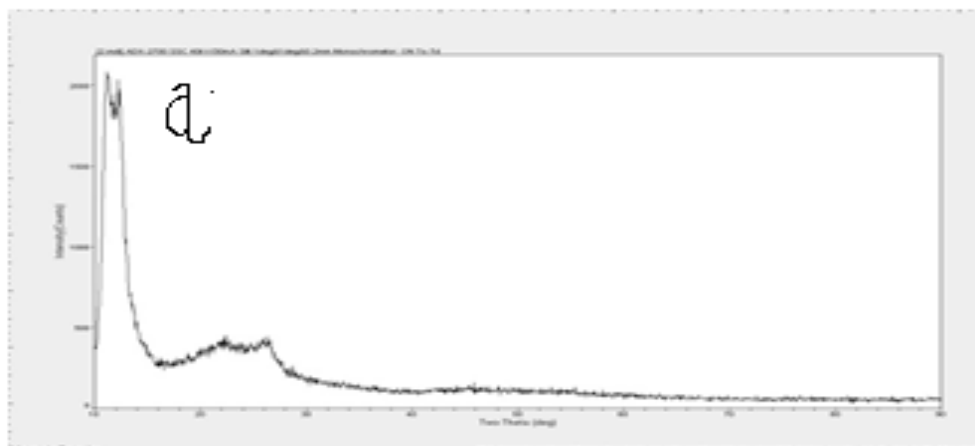
3.Results and Discussion

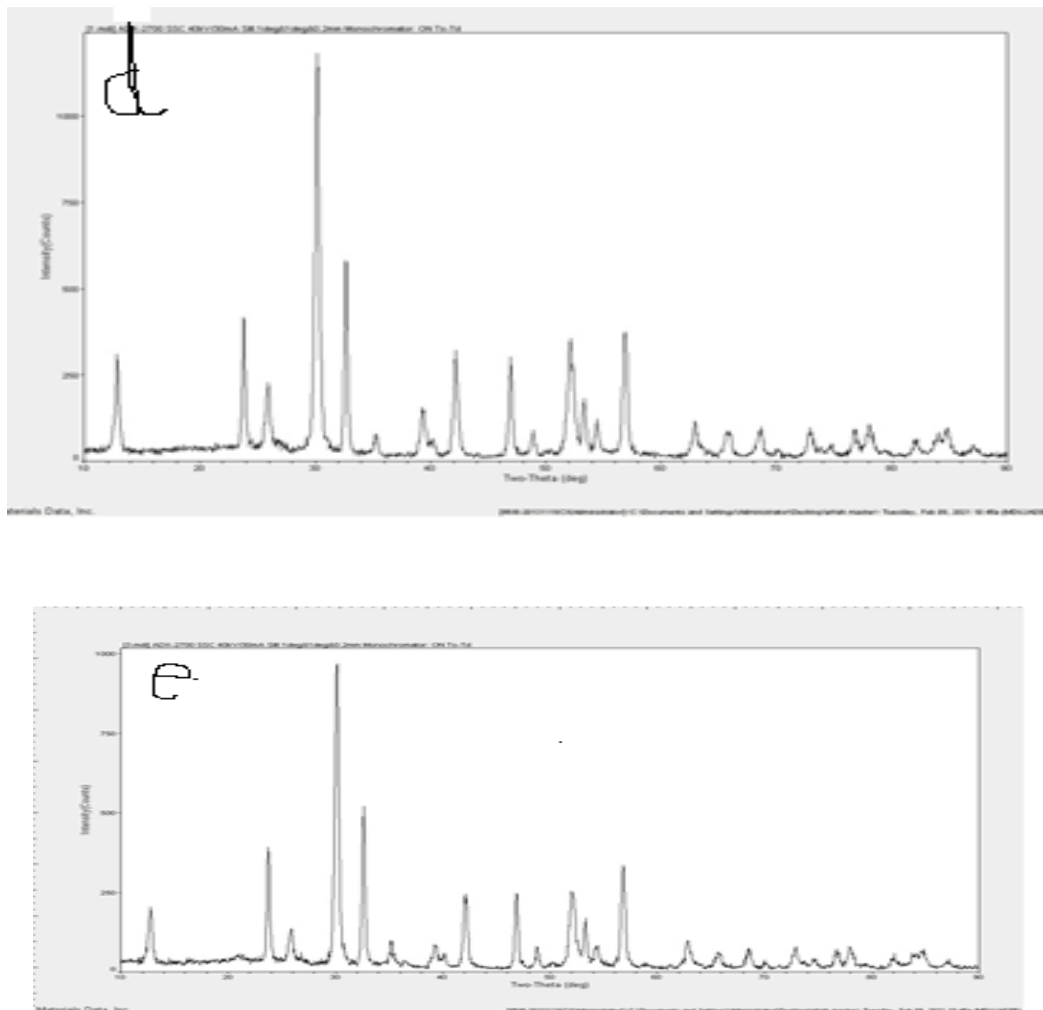
3.1 Characterization

a. X- Ray Diffraction: The XRD analyses of the graphine oxide (GO) nanosheets , Fe₃O₄ Nanoparticles, FGO Nanocomposite, TiO₂ Nanoparticles, and TFGO Nanocomposite in the range of 2 θ (10 - 90°) were appeared in figure 2. Figure (2a) shows the XRD analysis of GO nanosheets, the demise of a sharp band about (2 θ = 26°) from graphite exhibits the changing in the crystalline form of the graphite (Gr) and pointed to the destroying of the crystalline structure of Gr a big interlayer spacing arisen about to (8.12Å) at the diffracted angle (2 θ =11.152°) and other two peaks at (2 θ =23.88°) and (2 θ =43.68°)[11-14]. Figure (2b) shows the X-ray diffraction (XRD) spectrum of pure magnetic iron oxide Nanoparticles at diffraction angle and this (2 θ = 18.56,30.25, 35.69, 43.35, 53.54, 57.28 & 62.89°) corresponds to Previous studies (15) in this field, it was found that when

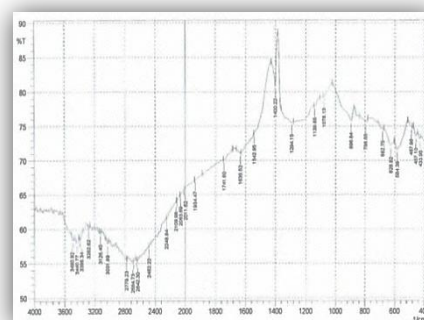
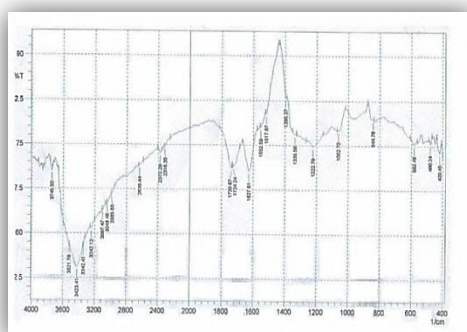
calculating the average size of crystals for the highest three peaks is about (51nm).

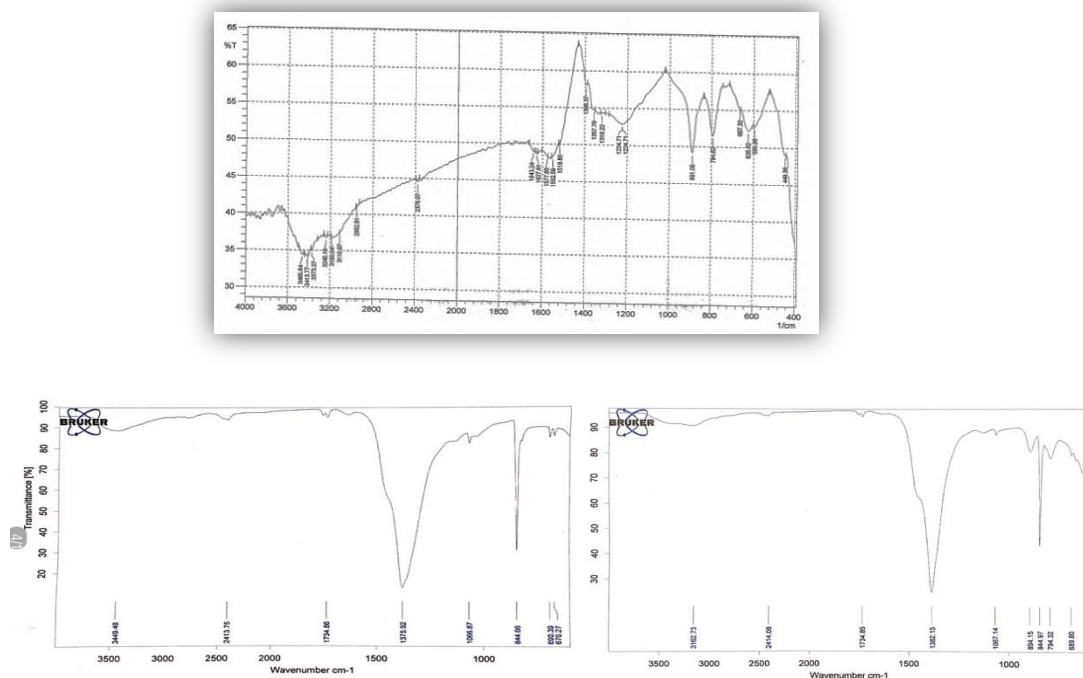
In Fig. (2c) compared to Fig. (2a), we note a decreases in the characteristic peak of graphene oxide and overpowered by strong signals for (Fe₃O₄) Nanoparticles, and this indicates the success of the local synthesis process for (Fe₃O₄) on graphene oxide sheets to obtain On the binary nanocomposite (FGO). By using the (Debye - Scherrer) equation [16], the average crystal size of the highest three peaks of the FGO was calculated and it was found about (60nm). Figure (2d) shows the X-ray diffraction analysis of TiO₂ Nanoparticles used in this study, where it was found that the peaks resulting from the diffraction angles are for the Anatase phase ($2\theta = 23.906, 30.295, 47.048, 52.245 \text{ \& } 56.995^\circ$) and the Rotyle phase ($2\theta = 26.040, 42.299 \text{ \& } 63.004^\circ$), this is consistent with previous studies (1 and 2). And by using the Debye - Scherrer equation to calculate the average crystal size for the highest three peaks of each phase for TiO₂ Nanoparticles under examination, it was found to be equal to the Anatase phase and the Rotyl phase (23.61, 28.14 nm) respectively[17]. Figure (2e) shows the similarity in the peaks of X-ray diffraction of pure titanium oxide nanoparticles with the (TFGO) nanocomposite, and with less intensity for all the diffraction peaks, and this is an indication of the success of the process of encapsulating the titanium oxide particles of the surface of the binary nanocomposite (FGO) to obtain the superposition .(TFGO) nanocomposite.





Figure(2): X-RD of a=GO Nanosheets, b=FO Nanoparticles, c=FGO Nanocomposites, d=TiO₂ Nanoparticles, e=TFGO Nanocomposites.





Figure(2): FT-IR Spectrum of a=GO Nanosheets, b=FO Nanoparticles, c=FGO Nanocomposites, d=TiO₂ Nanoparticles, e=TFGO Nanocomposites.

From figure (2a), it is noticed that several distinct peaks appear and include a wide absorption beam at about (3215.38 cm^{-1}), which is due to the stretch vibration of the OH group and the absorption of water on the surface of the graphene oxide plates, and we note the presence of absorption bands at ($1223.03, 1394.53\text{ cm}^{-1}$), which are due to the vibration of the stretch of homogeneous rings of the epoxy groups (COC), as well as the presence of a beam at about (1621.53 cm^{-1}) due to the presence of the non-oxidizing carbon composition ($\text{C} = \text{C}$). As for the peak at the frequency (1716.51 cm^{-1}), which is likely due to the vibration stretching the carbonyl groups ($\text{C} = \text{O}$), and the summit at the frequency (1045.83 cm^{-1}) may refer to the alkoxy group ($\text{C}-\text{OO}$), the presence of the previous two peaks indicating The presence of alkoxy and carbonyl groups on the edges of the plates, graphene oxide. The presence of the groups mentioned in the above discussion indicates that the graphite oxidation process took place and graphene oxide was obtained successfully[11-14].

The synthesized nanomaterials GO and G nanosheets, were investigated by (AFM), the results were almost identical as in figures(5) and with nanoparticles size about (25.7 nm)

The atomic force microscope (AFM) analysis measure the surface structure with high accuracy up to parts of the nanometer in addition to

measuring the granular size [11]. AFM analysis and the particle size distribution of (GO nanosheets) are shown in Figure 3 with size about (3 μm), and thickness of (94 nm). In a three-dimensional image of graphene oxide sheets, with a maximum height of the particles equal to (392.16 nm) and the average diameter of a Bags equal to (822.18 nm), as shown in both the table (1) and (Figure 3) the distribution of the values of the size of nanoparticles and platelets plan for the distribution of these plates respectively

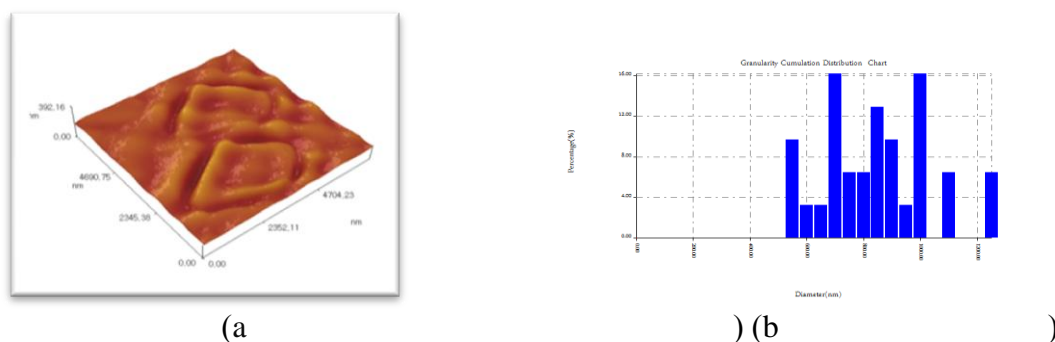


Fig. 3 shows AFM analysis for GO Nanosheets.

It is also possible to observe (AFM) examination of the iron oxide nanoparticles that were subsequently deposited on the surface of the graphene oxide as the maximum height of is (7.86 nm) as shown in Figure (4), and the prevailing diameter rate is equal to (70.63 nm), after depositing the nanoparticles of magnetic iron oxide on the surface of the graphene oxide we notice a change in the size of the particles as the maximum height of particles (34.41 nm) as shown in Figure (5), and that the dominant diameter of the nanocomposite (FGO) is equal to (80.43 nm) as shown in Figure (5).

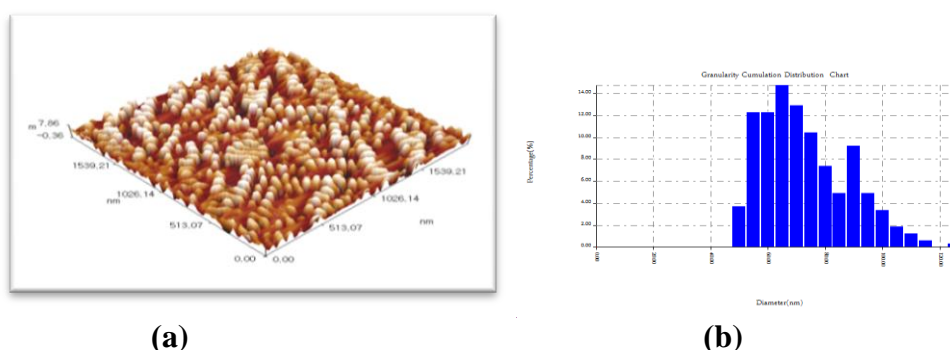
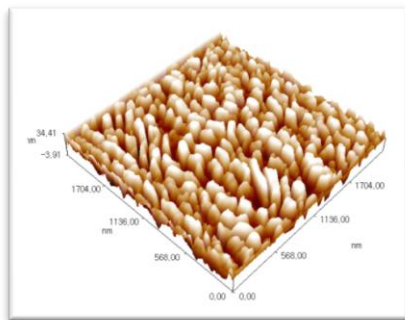
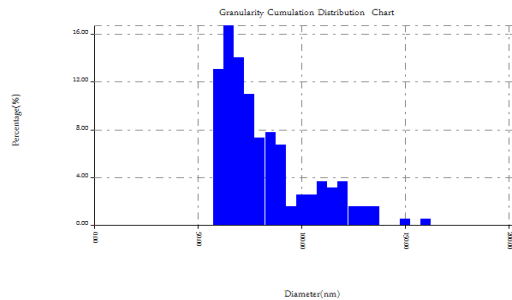


Fig. 4 shows AFM analysis for Fe₃O₄ Nanoparticles



(a)



(b)

Fig. 5 shows AFM analysis for FGO Nanocomposite.

Figure (6) shows a three-dimensional image of TiO_2 nanoparticles, as the maximum height of particle is (96.40 nm), and its prevailing diameter is equal to (50.55 nm) and Figure (6), But in Figure (7), we notice a change in the size of the particles, as the maximum height is (5.92 nm), and the dominant diameter of the compound (142.38 nm).

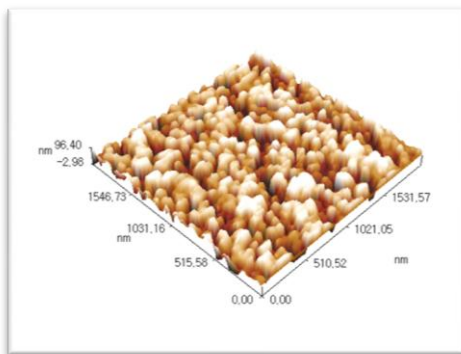
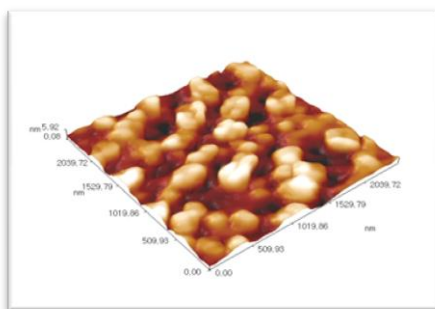
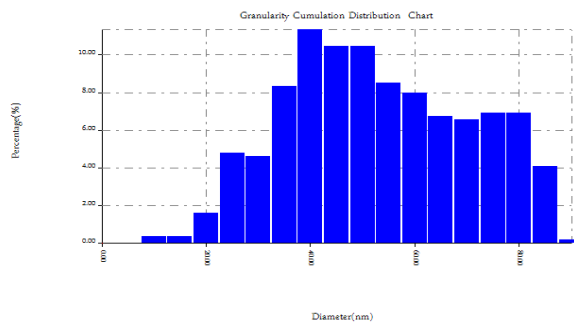
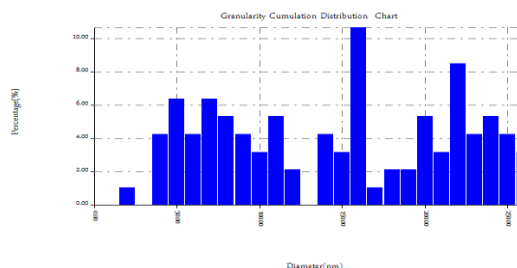


Fig. 6 shows AFM analysis for TiO_2 Nanoparticles.



(a)



(b)

Fig. 7 shows AFM analysis for TFGO Nanocomposite.

3.2. Photo Degradation Efficiency

The photo degradation of CR dye in existence of TFGO nanocomposite as photocatalyst agents was studied under solar light energy. The residue amount of CR dye in the reaction blend was calculated by using spectrophotometer. The results gained for the degradation of CR dye be seen in Figures 8, 9. The eminent degradation of CR dye was in 320 min study in the existence of TFGO nanocomposite in comparison to the other photocatalyst agents. Photocatalytic processes experiments were happen at different like effects of Photocatalysis, temperatures and existence of sun light. The removal efficiency of TFGO nanocomposite was calculated using equation[12]:

$$R\% = (C_0 - C_t / C_0) * 100$$

C_0 , C_t are initial and final concentration of CR dye in the solution, then the results tabulated in table 1

Table 1: The Photocatalytic Data of TFGO nanocomposite as photocatalyst

T(min)	T(298K)			T(308K)			T(318K)		
	C_t	C_t/C_0	R%	C_t	C_t/C_0	R%	C_t	C_t/C_0	R%
-60	9.7509	1	0	9.7509	1	0	9.7509	1	0
0	7.7787	0.7977	20.2259	7.4361	0.7626	23.7394	7.1583	0.7341	26.5881
120	5.9453	0.6097	39.0276	5.1120	0.5243	47.5738	4.5102	0.4625	53.7461
240	4.7139	0.4834	51.6570	4.2879	0.4397	56.0251	2.8528	0.2926	70.7435
360	4.3806	0.4492	55.0754	2.8620	0.2935	70.6486	2.4269	0.2489	75.1116
480	3.1306	0.3210	67.8948	1.9361	0.1985	80.1443	1.0935	0.1121	88.7855
600	2.5565	0.2622	73.7822	1.0935	0.1121	88.7854	0.7231	0.0742	92.5838

3.2.1. The Role of Graphene Oxide GO Nanosheets on The Photocatalytic Activity

The photocatalytic mechanism of the TGs nanocomposites is suggested in the following steps:

The first step: This is the adsorption of the phenol molecule on the high surface of graphene oxide nanosheets. Upon interaction with graphene oxide nanosheets, the oxidative species surrounding the catalyst can readily access the adsorbed CR dye, making the photodegradation process more effective.

The second step: Under visible-light irradiation, p state electrons were excited in the graphene oxide nanosheets by absorbing visible-light.

Owing to the p–d conjugate, the p state electrons were subsequently injected into the conduction band of TiO₂ nanoparticles [13–47]. The high carrier mobility of graphene oxide nanosheets makes the photogenerated electrons transfer to TiO₂ nanoparticles quickly, which is in favor of utilizing efficiency of photogenerated electrons and high photoactivity. These electrons transferred to the surface of TiO₂ nanoparticles and reacted with oxygen to yield superoxide and hydroxyl radicals.

The third step: In the presence of graphene oxide nanosheets, the excited electrons are quickly transferred through the sp²-hybridized network of graphene oxide nanosheets. If the electron–hole pairs are prevented from recombining, the excited electrons on the valence band will be available to reach the reaction points and generate oxidative species, thus enhancing the performance of photocatalytic processes.

3.2.1.The Factors Affecting On The Photocatalytic Activity

a. Effect of presence of sun Light

The photodegradation reaction of CR dye in existence of TFGO nanocomposite as photocatalyst was studied at presence of sun light or at the dark. From the results which exhibit in Figure 24 that shown the TFGO nanocomposite at the presence of sun light are proving as an more efficient photocatalyst for the degradation of CR dye compared with putting CR dye solution at dark

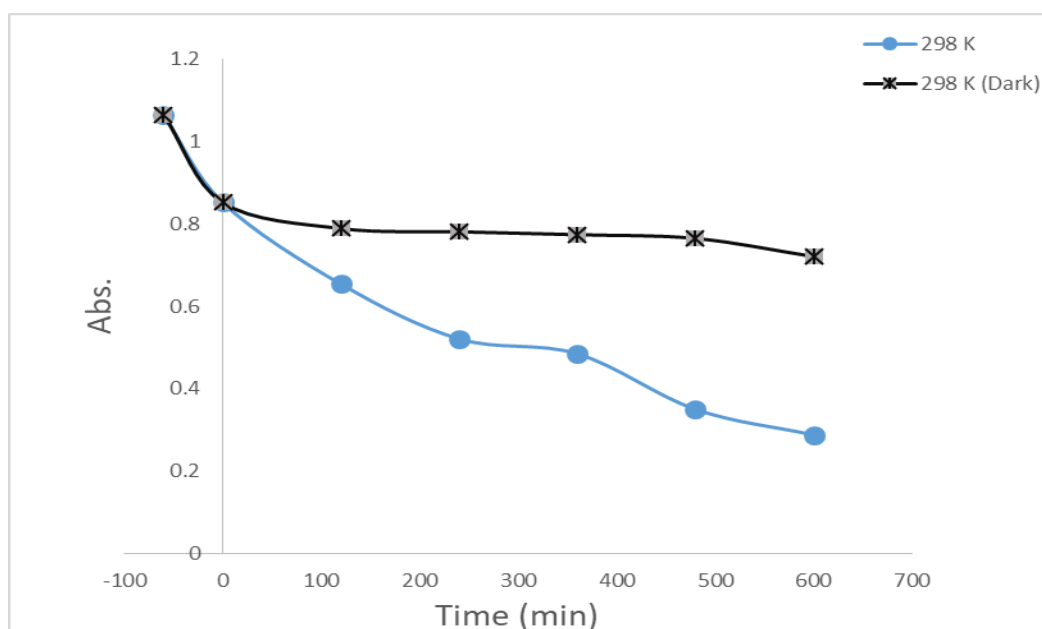


Figure 8 The photo degradation of CR dye in existence of TFGO nanocomposite as photocatalyst with and without light.

b. Effect of Temperatures

The photodegradation reaction of CR dye solution in existence of TFGO nanocomposite as photocatalyst was also carried out under varying temperature conditions from (298 to 318k), (Figure 9). The percentage of Photodegradation efficiency was found to very low at 298k for TFGO nanocomposite, and then increases at 308k, and then at 318 k, this is due to the increase in the speed of the photodegradation reaction with increasing temperatures.

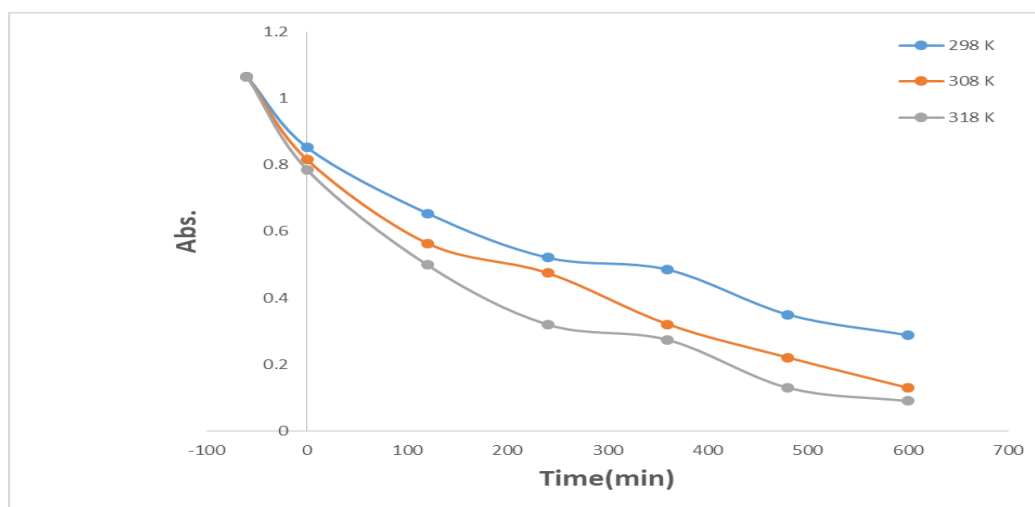


Figure 9: The photo degradation of CR dye in existence of TFGO nanocomposite as photocatalyst at different temperatures.

4. Conclusion: The purpose of this article was to describe that, prepared FGO and TFGO nanocomposite from limited amount of GO nanosheets, F_3O_4 nanoparticles, TiO_2 nanoparticles. The prepared materials and components were characterized by using many advises like (FTIR) and (AFM). The performance of prepared materials and components as photocatalyst was investigated by applying them in advanced oxidation processes (AOP) to degradation of CR dye under solar light. The photodegradation efficiency of CR dye could be gained 92% at existence of TFGO nanocomposite as photocatalyst within 600 min. Photocatalytic processes experiments were happen at different effects like Photocatalysis, temperatures and existence of sun light.

References

- [1] L. Musab, and E. E. Al- Abodi "Preparation and Characterization Composites Contain of Magnetic Iron Oxide Nanoparticles with Different Weight Ratios of Dextrin , and Using it to Removal of Heavy Metals from Aqueous Solutions", *Energy Procedia* 157(2019) 752-762.
- [2] A.Jawad and E.E. Alabodi " Investigating (Fe₃O₄) Magnatic Nanoparticles Impregnated onto Tri-sodium citrate to Remove, of methylene blue dye from Aqueous Solutions", *AIP Conference Proceedings* 2123, 020026 (2019).
- [4] Y.M.Sadiq, and E. E. Al- Abodi "Preparation and Characterization of Anew Nano Mixture and Its Application as Photocatalysis in Self-Assembly Method for Water Treatment", *AIP Conference Proceedings* 2190, 020042 (2019).
- [5] S.A. Khanosh and E. E. Al- Abodi "Using Advanced Oxidation Processes (AOP) to Remove BCB Dye Pollutants From Waste Water" *AIP Conference Proceedings* (2021) under printing.
- [6] APHA, 2005. Standard methods for the examination of water and waste water, 21 ed. American Water Works Association and Water Environment Federation.
- [7] Kansal, S.; Kaur, N.; Singh, S. "Photocatalytic degradation of two commercial reactive dyes in aqueous phase using nanophotocatalysts ," *Nanoscale Res. Lett.* 2009, 4, 709–716.
- [8] Mehra, M.; Sharma, T.R. "Photocatalytic degradation of two commercial dyes in aqueous phase using photocatalyst TiO₂ ," *Adv. Appl. Sci. Res.* 2012, 3, 849–853.
- [10] Hummers W S and Offeman R E, 1958, *J. Am. Chem. Soc.* **80** 1339
- [11] A. Farouk, I. Latifand and E. E. Al- Abodi, (2016) "Preparation and Characterization of Silver Nanoparticles and Study Their effect on the Electrical Conductivity of the Polymer Blend(Poly vinyle acitet. Pectin ,poly Aniline)", *Ibn Al-Haitham Jour. for Pure & Appl. Sci.* Vol. 29 (3).
- [12] E. Alobodi, A. Farouk" Preparation Characterization and Electrical Study of Polymeric Mixture Nanocomposites ", *International Journal of Advanced Research in Science, Engineering and Technology* Vol. 3, Issue 2, February(2016)
- [13] E. Alobodi, A. Farouk, (2018) " Preparation Characterization and Electrical Study of New Polymeric Mixture (Consist of Three Polymer Nanocomposites) ", *IOP Conf. Series: Journal of Physics: Conf. Series* Vol. 1003, Issue 012014.
- [14] E. E. Al- Abodi, I. Latifand A. Farouk ,(2018) Iraqi Patent No. Y10S977/73 C08J5/10 Baghdad, Iraq: central Organization for Standardization and Quality Control.
- [17] J. O. Carneiroa, G.Vasconcelos, S. Azevedoa, C. Jesus, C. Palhac, N. Gomes, V. Teixeira,(2014)"The evaluation of the thermal behaviour of a mortar based brick masonry wall coated with TiO₂ nanoparticles: An experimental assessment towards energy efficient buildings" *Energy and Buildings*,8,1-8 DOI: [10.1016/j.enbuild.2014.06.006](https://doi.org/10.1016/j.enbuild.2014.06.006)
- [11] Ezhkova A. M., Yapparov A. Kh., Ezhkov V. O., Yapparov I. A., Sharonova N. L., Degtyareva I. A., Khisamutdinov N. Sh., Bikkinina L. M. Kh.," Fabrication of Nanoscale Bentonite, Study of Its Structure And Toxic Properties, And etetermination of Safe doses",*Nanotechnologies in Russia* 10.1-2, 120-127, (2015).
- [12] Rauf M.A. and Ashraf S.S. 2009 Fundamental principles and application of heterogeneous photocatalytic degradation of dyes in solution. *Chem Eng J* **151**:10. <http://dx.doi.org/10.1016/j.cej.2009.02.026>.

- [13] Y. Liang, H. Wang, H.S. Casalongue, Z. Chen, H. Dai, Nano Res. 3 (2010) 701–705.
- [14] Y. Wang, R. Shi, J. Lin, Y. Zhu, Appl. Catal. B 100 (2010) 179–183.
- [15] F. Zhao, B. Dong, R. Gao, G. Su, W. Liu, L. Shi, C. Xia, L. Cao, Appl. Surf. Sci. 351 (2015) 303–308.
- [16] J. Liu, H. Bai, Y. Wang, Z. Liu, X. Zhang, D.D. Sun, Adv. Funct. Mater. 20 (2010) 4175–4181.
- [17] D. Yoo, T.V. Cuong, V.H. Pham, J.S. Chung, N.T. Khoa, E.J. Kim, Curr. Appl. Phys. 1 (2011) 805–808.